Tempering of Steel

G. R. SPEICH AND W. C. LESLIE

Tempering of martensitic steels involves the segregation of carbon, the precipitation of carbides, the decomposition of retained austenite, and the recovery and recrystallization of the martensitic structure. Because these several reactions overlap and occur on such a fine scale, it is only recently that our knowledge of the resulting structures has become reasonably complete. Our present understanding of the processes involved in the tempering of iron-carbon martensites and how they are affected by alloying elements is reviewed.

TEMPERING is the process of heating martensitic steels to elevated temperatures so that they become more ductile. It involves the segregation of carbon to lattice defects and the precipitation of carbides, the decomposition of retained austenite, and the recovery and recrystallization of the martensitic structure. These several reactions often overlap and they occur on a very fine scale, so it is only since the advent of transmission electron microscopy in 1956 that our knowledge of the structures of tempered martensite has become reasonably complete.

Each of the processes involved may be affected by alloying additions so that the tempering behavior of alloy steels becomes a fascinating but complex subject. In addition, interaction of trace elements with former austenite grain boundaries during tempering may promote embrittlement. Obviously, these subjects are too large to treat in detail in this short review. Rather, we treat the basic tempering processes in iron-carbon martensites and then illustrate how these basic processes can be altered by alloying elements.

E. C. Bain was closely interested in the tempering of steels during his entire career. He coauthored a paper on high-speed steels in 1931 with M. A. Grossmann much of which was concerned with the secondary hardening of high-alloy steels.[1] In his famous book on alloying elements in steels[2] he devoted a large section to discussing the effect of alloying elements on tempering. In his Eighth Hatfield Memorial Lecture before the Iron and Steel Institute[3] he discussed the structure and tempering of martensite as it was understood in 1955. It is only fitting that we review our present understanding of the tempering of martensite in celebration of his 80th birthday.

STRUCTURE OF UNTEMPERED MARTENSITE

A review of tempering should begin with our present understanding of the structure of untempered martensite since this is the matrix in which the tempering processes occur. In steels the parent phase is nearly always austenite with a fcc structure, but the daughter phase may have a bcc, bct, or hcp* crystal structure.

*fcc = face centered cubic, bcc = body centered cubic, bct = body centered tetragonal, hcp = hexagonal close packed crystal structure.

Lath martensite† is the most commonly occurring martensitic structure; its appearance is illustrated in Fig. 1. It is typical of all low- and medium-carbon martensites. The crystal structure of lath martensite is usually bcc, although in low-alloy steels with more than 0.2 pct C bct martensite is formed. The martensite units form in the shape of laths, grouped into larger sheaves or packets. The substructure consists of a high density of dislocations arranged in cells; each martensite lath is composed of many dislocation cells with an average width of 2500Å.[4,5] Typical dislocation densities are estimated to be 0.3 to 0.9 $\times 10^{12}$ cm/cm^3. The substructure is superficially similar to that developed in iron by heavy cold work.[6]

†Alternative nomenclature is massive martensite, dislocated martensite, or low-carbon martensite.

G. R. SPEICH and W. C. LESLIE are associated with the Research Laboratory, U. S. Steel Corp., Monroeville, Pa.

A different type of martensite predominates in high-carbon steels and in iron-base alloys with M_S temperatures below ambient.[4,5] This is *plate martensite* and its structure is illustrated in Fig. 2. Its crystal structure may be either bct or bcc. The martensite units form as individual lenticular plates. The substructure of plate martensite consists of very fine twins with a spacing of about 50Å. These twins generally do not extend to the sides of the plates, but degenerate into a complex dislocation array near the periphery of the plate.[4,5]

Medium-carbon steels may contain a mixture of lath and plate martensite so their structure is unusually complicated, as illustrated in Fig. 3. The ratio of volume fraction of lath martensite to volume fraction of plate martensite in Fe-C alloys with various carbon contents is given in Fig. 4. The amount of retained austenite at room temperature and the M_S temperature of these Fe-C alloys are also given. The relative amounts of plate martensite are increased when elements such as nickel are added which lower the M_S temperature.

CARBON SEGREGATION

Most steels have M_S temperatures above ambient. Therefore, when they are quenched, there is some brief period in which carbon atoms can redistribute themselves. This process is called quench-tempering or auto-tempering. Because of the stress fields around individual dislocations and cell walls in lath martensite, certain interstitial lattice sites near these defects provide lower-energy sites for carbon than the normal interstitial lattice positions.[10] Obviously, the same mechanism operates here as in the strain-aging of iron, a field extensively reviewed by Baird.[11] Also, when martensite is tempered at low temperatures, the first step in the tempering process is a redistribution of carbon to these lower energy sites. In many low-

carbon steels, because of their high M_S temperatures, Fig. 4, this carbon redistribution has already occurred during quenching through the martensite temperature range. We cannot detect such segregation by metallography, but we can detect it by the smaller contribution of carbon to electrical resistivity or to internal friction when carbon is an interstitial site near a dislocation than when it is in a "normal" interstitial lattice site.[12] This effect is illustrated in Fig. 5. A series of eight Fe-C alloys, in the form of 0.010 in. thick sheet, were austenitized in vacuum and quenched into iced brine. The quenching rate was sufficiently high so that all the alloys transformed completely to martensite and no carbide precipitated during quenching. Specimens were then put into liquid nitrogen and the resistivity was measured. The resistivity can be separated into two distinct regions. In the first, extending from 0 to 0.20 pct C, the contribution of carbon to electrical resistivity is 10 $\mu\Omega$ cm/wt pct C, whereas in the second the contribution is three times as great, about 30 $\mu\Omega$ cm/wt pct C. The lower specific electrical resistivity in the low-carbon region results from the segregation of carbon to dislocations during quenching. With carbon contents below 0.2 pct, Speich[12] has calculated that nearly 90 pct of the carbon is segregated to lattice defects during quenching. Above 0.20 pct C, such sites become nearly saturated and carbon atoms are held in the "defect-free" lattice. It is interesting to note that 0.20 pct C is also about the carbon content at which tetragonality in martensite is first detected; this segregation of carbon to defects can explain the lack of tetragonality at carbon contents below 0.2 pct. Alternative proposals for this lack of tetragonality involve a disordering of the carbon atoms below 0.2 pct.[13]

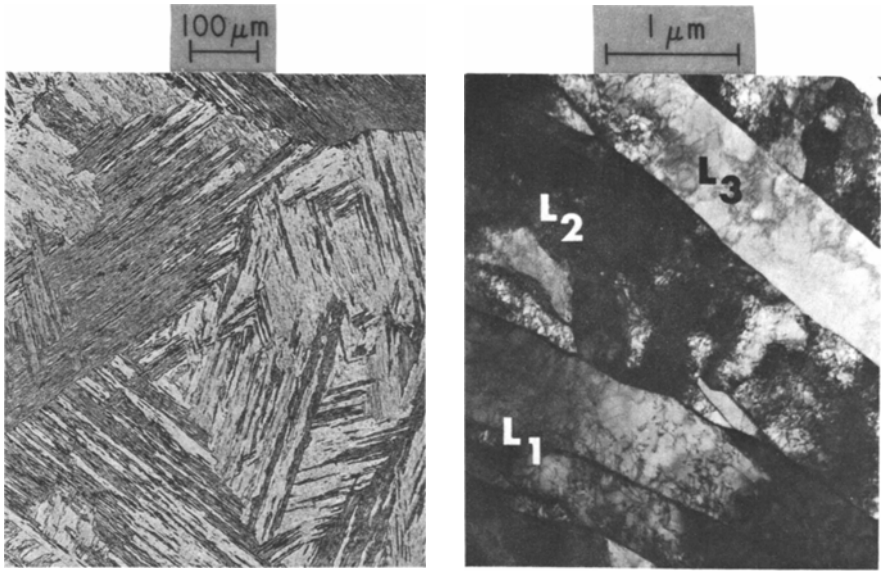

Fig. 1—Structure of lath martensite in 0.02 pct C, 2 pct Mn steel. (*a*) Light micrograph, (*b*) electron transmission micrograph (L_1, L_2, L_3 represent separate laths; the laths are separated by high-angle boundaries but each lath may contain many low-angle dislocation cells.

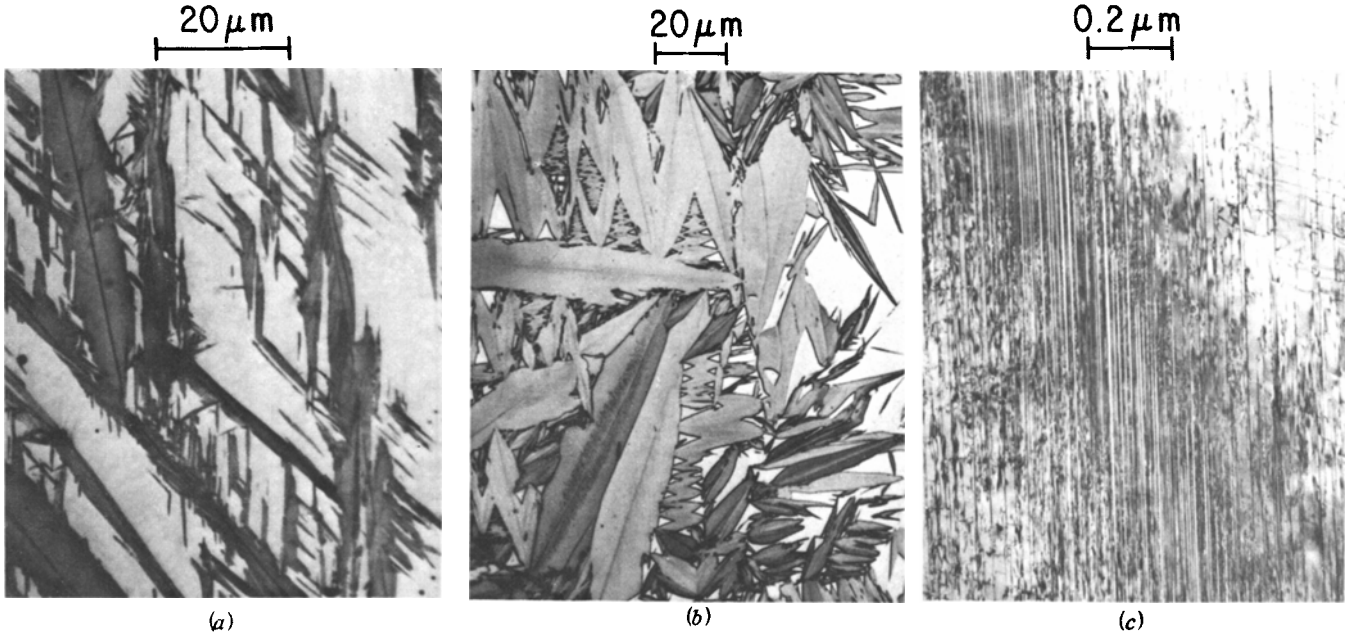

Fig. 2—Structure of plate martensite: (*a*) 1.2 pct C steel, light micrograph; (*b*) Fe-30 pct Ni alloy, light micrograph; (*c*) Fe-30 pct Ni alloy, electron transmission micrograph.

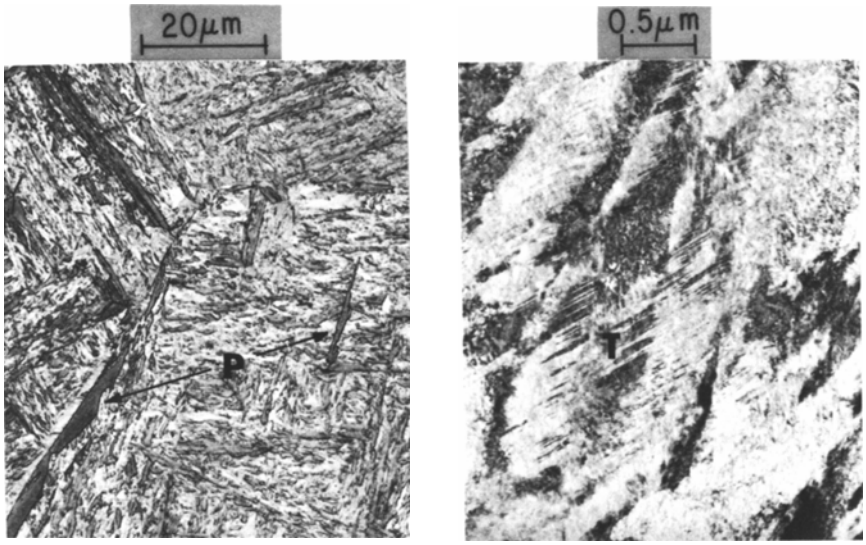

Fig. 3—Mixed lath and plate martensite structure in 0.57 pct C steel: (*a*) light micrograph, (*b*) electron transmission micrograph (plate martensite labelled P; twinned substructure labelled T).

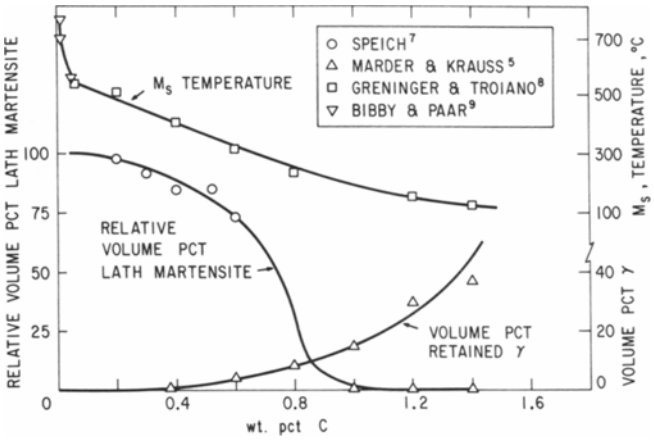

Fig. 4—Effect of carbon content on relative volume percent of lath and plate martensite, M_s temperature, and volume percent of retained austenite in Fe-C alloys.

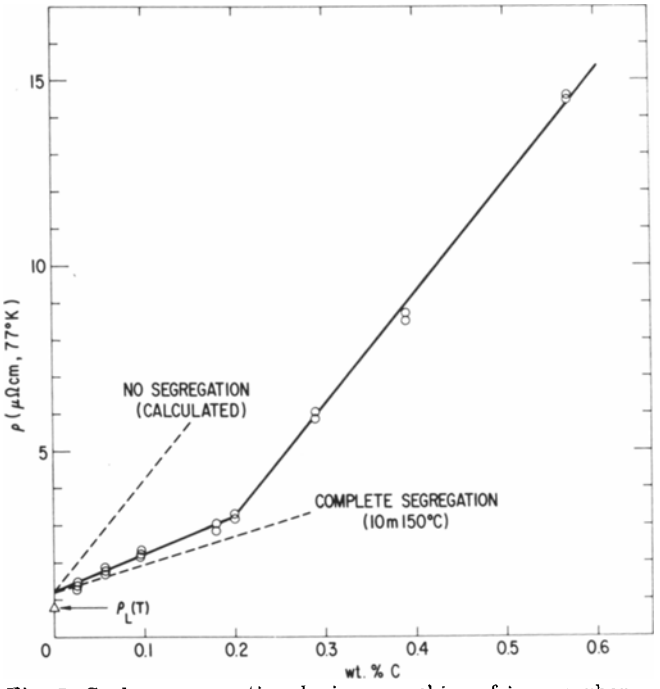

Fig. 5—Carbon segregation during quenching of iron-carbon martensites as detected by electrical resistivity measurements.[12]

Kurdjumov and coworkers[14,15] have studied the segregation of carbon to defects in high-nickel, low-carbon martensites with low M_S temperatures by measuring the amplitude dependence of internal friction at liquid nitrogen temperatures after annealing such martensites at room temperature. The amplitude dependence of internal friction after annealing various periods at room temperature is shown in Fig. 6. The slope of the lines in Fig. 6 (labelled α) is a measure of the amplitude dependence of the internal friction. Since the main contribution to internal friction at liquid nitrogen temperatures is dislocation damping, a decrease in Q^{-1} indicates carbon pinning of dislocations. In addition, the decrease in the amplitude dependence of $Q^{-1}(\alpha)$ has been attributed by Kurdjumov[14] to segregation of carbon to dislocations, because the same decrease in α occurs during strain aging of iron deformed 5 pct.[16] Similarly, in low-carbon, iron-carbon martensites with high M_S temperatures this carbon segregation is completed during quenching. The Snoek peak for these steels, Fig. 7, indicates a very low value compared to a low-carbon "defect-free" iron of the same carbon content.[12] Even when the carbon content is increased to 0.18 pct, the value of the Snoek peak is still lower than in the 0.026 pct C "defect-free" iron, indicating that most of the carbon is segregated during quenching, as indicated by electrical resistivity. These measurements, as those of Kurdjumov, indicate that carbon is pinned to dislocations and Snoek jumps are prevented; thus, the height of the Snoek peak is decreased. Since carbon can diffuse during the measurements, the Snoek peak is lowered when the specimens are cooled (see 0.18 pct C data). The value of α decreases with increasing carbon content up to 0.2 pct C, above which it remains constant, as shown in Fig. 8. This is interpreted as indicating again that dislocations in martensite are saturated at 0.2 pct C, curve 1, Fig. 8. In annealed iron, curve 2, Fig. 8, saturation of dislocations occurs at much lower carbon levels because of the lower dislocation density.

In high-carbon steels, or in high-alloy, low-carbon

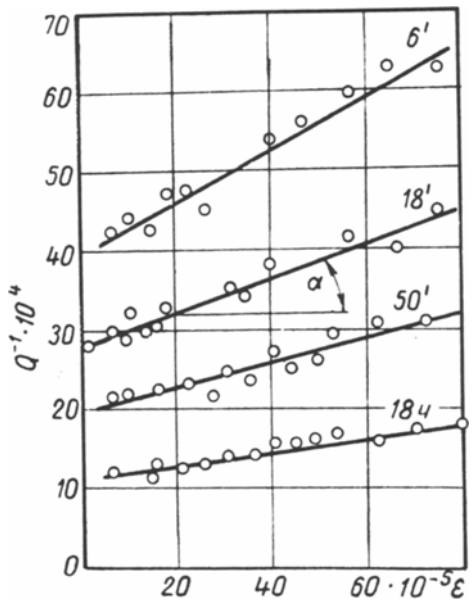

Fig. 6—Amplitude dependence of internal friction in Fe-29 pct Ni-0.16 pct C martensite aged various periods at 25°C (77°F).[15] (Q^{-1} is the internal friction, ϵ is the strain amplitude, and α is the rate of change of Q^{-1} with ϵ.)

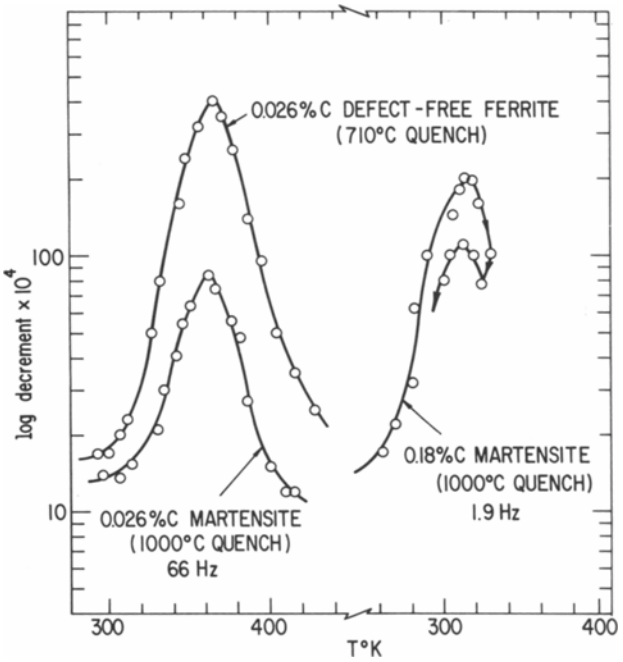

Fig. 7—Internal friction of low-carbon, iron-carbon martensites and "defect-free" α iron.[12]

steels containing plate martensite with internally twinned substructure, fewer of these low-energy dislocation sites are available. In these circumstances, carbon segregation to dislocations is not the only segregation reaction. Mössbauer studies[17] indicate that preprecipitation clustering of carbon also occurs. In this case, the electrical resistivity contribution of carbon is increased because of the stress fields created by the clusters.[18] It is usually necessary to study such reactions below room temperature in steels with low M_S temperatures since most of the clustering is completed by the time specimens are heated to room temperature, as indicated by the work of Winchell and

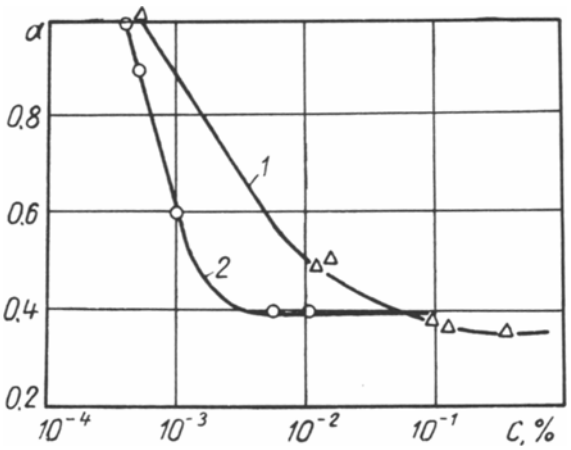

Fig. 8—Variation of amplitude dependence of internal friction with carbon content in Fe-29 pct Ni martensite.[15] (Curve 1 martensite; Curve 2 "defect-free" α iron; α is the rate of change of Q^{-1} with strain amplitude.)

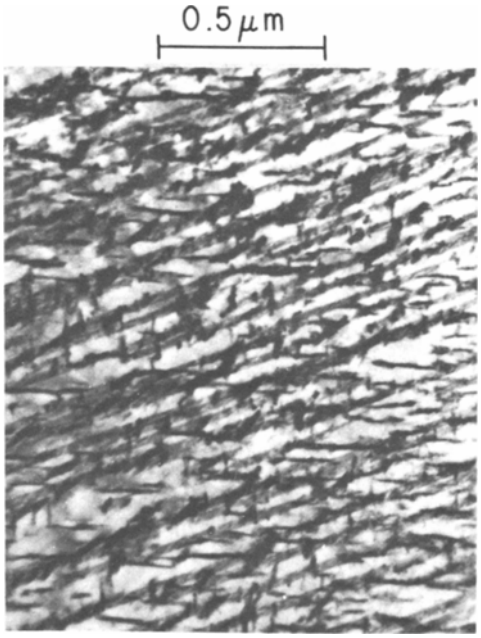

Fig. 9—Precipitation of ϵ-carbide in Fe-24 pct Ni-0.5 pct C martensite tempered 30 min at 205°C (401°F).[24]

Cohen.[18] Although the use of low-M_S steels is helpful in such studies because it avoids quench-tempering, the structure is changed from lath martensite to plate martensite. It is not yet clear whether preprecipitation clusters are ever present in commercial low-carbon or medium-carbon steels, which are principally lath martensite with a high density of dislocations. Unfortunately, no investigator has been able to produce the lath martensite structure in an alloy with an M_S temperature below room temperature.

Izotov and Utevskii[19] have detected early stages of decomposition of tetragonal high-carbon martensite by the formation of nodes in electron diffraction patterns. They have interpreted such nodes as resulting from a clustering of carbon atoms along {001} planes and distributed on one of the three sets of interstitial sublattices which lead to tetragonality. Subsequent heating to 100°C (212°F) or higher leads to the growth of the clusters and the eventual formation of ϵ-carbide.

This preprecipitation clustering process has been discussed theoretically by Khachaturyan[20] and by Johnson.[21,22] The driving force is a lowering of the total elastic energy of the lattice, as discussed recently by Hoffman.[23]

CARBIDE PRECIPITATION

When steels containing more than about 0.2 pct C are tempered at temperatures between 100°C (212°F) and 200°C (392°F), ϵ-carbide ($Fe_{2.3}C$, hcp) is the first carbide precipitated, as shown in Fig. 9. This process is often referred to as the first stage of tempering, but this is a misnomer, since carbon segregation or preprecipitation clustering precedes it.

The habit plane of ϵ-carbide has been shown by Wells[24] to be $\{100\}_M$ although the carbides appear to form preferentially on one set of the three possible $\{100\}_M$ planes. The orientation relation between α-iron and ϵ-carbide is reported by Wells as $(011)_M \| (0001)_\epsilon$ and $(101)_M \| (10\bar{1}1)_\epsilon$. The metastable carbide precipitated in α-iron at 100° to 150°C (212° to 302°F) also precipitates on $\{100\}_\alpha$ although there has been disagreement whether this carbide is ϵ-carbide, because in the Fe-N system a nitride similar in morphology and habit plane has been shown to be $Fe_{16}N_2$ (bct). Recent work by Langer[25] does, however, identify this carbide as ϵ. The morphology of this carbide is shown in Fig. 10 and the three sets of $\{100\}_\alpha$ planes are clearly delineated.[26]

In low-alloy steels containing less than 0.2 pct C the precipitation of ϵ-carbide is inhibited during tempering at 100° to 200°C (212° to 392°F). As mentioned before, most of the carbon in these steels is at dislocation sites. Most of these sites have a lower energy than those available in ϵ-carbide, so there is little driving force for precipitation.[10] Before precipitation can occur some dislocations must be removed by recovery, but the presence of carbon strongly inhibits recovery, so we have a delicately balanced situation.

Fig. 11 shows the progress of tempering of low-C, Fe-C alloys at 150°C (302°F), as measured by electrical resistivity.[12] The region marked A is associated with the continued segregation of carbon to defects in the martensite that began during quenching. Region C is associated with ϵ-carbide precipitation, and B is a transition region. Below 0.18 pct C, carbide precipitation is very sluggish at 150°C (302°F), in contrast to tempering of "defect-free" α-iron in which carbide precipitation is detected at 60°C (140°F) after 1 hr, as shown in Fig. 12.[27] When the carbon content of martensite is increased to 0.4 pct, the electrical resistivity continuously decreases with time at all temperatures, with no indication of three distinct regions. At these higher carbon contents not all the carbon can be associated with dislocations and carbide precipitation occurs rapidly even at 150°C (302°F).[12]

Hägg carbide (Fe_5C_2, monoclinic) is apparently formed in some high-carbon steels tempered at 200°

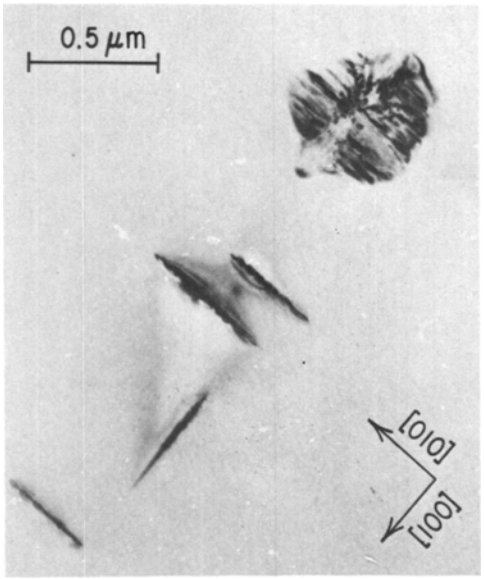

Fig. 10—Metastable carbide precipitation on $\{100\}_\alpha$ planes in an Fe-0.013 pct C alloy quenched from 700°C (1292°F) and aged 6 hr at 200°C (392°F).[26]

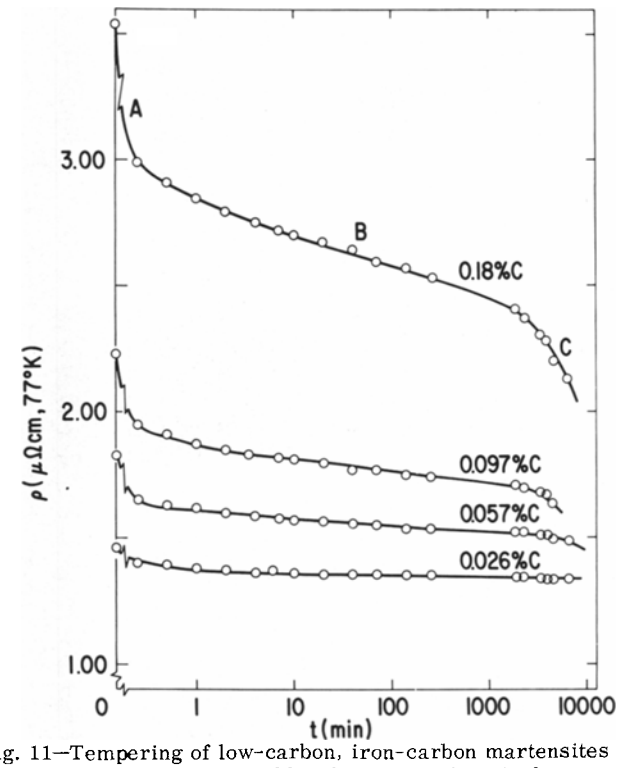

Fig. 11—Tempering of low-carbon, iron-carbon martensites at 150°C (302°F) as indicated by changes in electrical resistivity.[12]

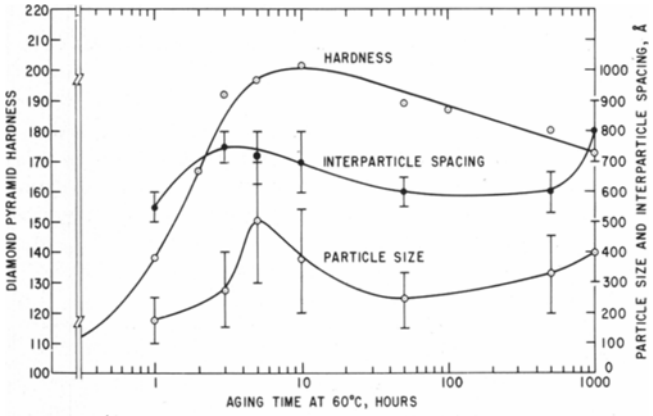

Fig. 12—Change of hardness, interparticle spacing, and particle size during aging of 0.03 pct C rimmed steel at 60°C (140°F).[27]

Fig. 13—Precipitation of Fe_3C in Fe-0.39 pct C martensite tempered 1 hr at 300°C (572°F).[12]

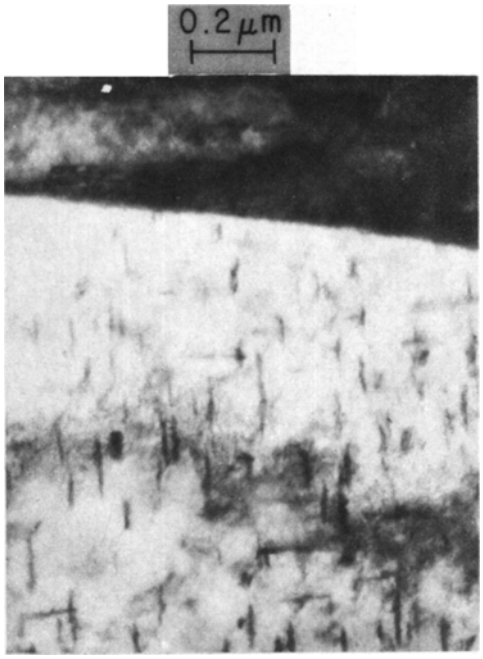

Fig. 14—Precipitation of Fe_3C during quenching in AISI 4315 steel.[7]

to 300°C (392° to 572°F), according to evidence from recent Mössbauer studies.[28] It is a metastable carbide intermediate between ϵ and cementite. In low-carbon steels we are uncertain whether Hägg carbide appears in the tempering sequence because the diffraction patterns from cementite and Hägg carbide are similar,[29] and no Mössbauer data are available.

Cementite (Fe_3C, orthorhombic) forms when most steels are tempered to 250° to 700°C (482° to 1292°F). This is sometimes called the third stage of tempering, the second stage being the decomposition of retained austenite. The initial morphology of cementite in martensite is needle-like when formed either during deliberate tempering, as shown in Fig. 13, or when formed during the quenching of large sections, as shown in Fig. 14. The nucleation sites are frequently martensite lath boundaries at low temperatures and ferrite grain boundaries at higher temperatures. Wells[24] has shown that in a 24 pct Ni, 0.5 pct C steel the orientation relation of Fe_3C with α-iron is $(112)_M \| (001)_{Fe_3C}$; $[11\bar{1}]_M \| [010]_{Fe_3C}$; $[1\bar{1}0]_M \| [100]_{Fe_3C}$. The habit plane in the martensite is $\{112\}_M$, the twinning plane. A fine structure is frequently observed in the cementite and consists of needles parallel to the $[010]_{Fe_3C}$ direction and the $[111]_M$ direction. Similar results have been reported by Leslie *et al.*[30] for precipitation of Fe_3C in "defect-free" iron; the fine structure of the Fe_3C is shown in Fig. 15 and the orientation relation is shown in Fig. 16. As the tempering temperature is increased this plate-shaped Fe_3C gradually spheroidizes to reduce surface energy. At 700°C (1292°F) the final structure consists of Fe_3C spheroids in a "defect-free" α-iron matrix.

Alloy carbides that form at 500°C (932°F) and 600°C

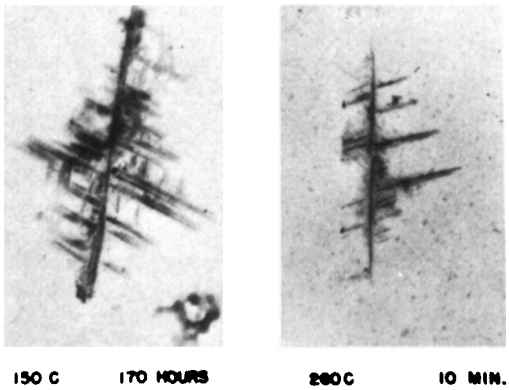

Fig. 15—Precipitation of Fe_3C in Fe-0.014 pct C alloy quenched from 740°C (1364°F) and aged as shown.[30]

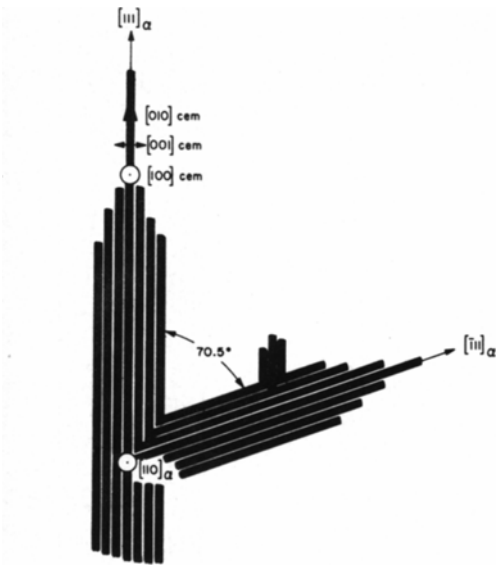

Fig. 16—Orientation of growth of dendritic cementite in ferrite.[30]

Fig. 17—Recovered structure of Fe-0.18 pct C martensite tempered 10 min at 600°C (1112°F) (light micrograph).[12]

Fig. 18—Recovered structure of Fe-0.18 pct C martensite tempered 10 min at 600°C (1112°F) (electron transmission micrograph).[12]

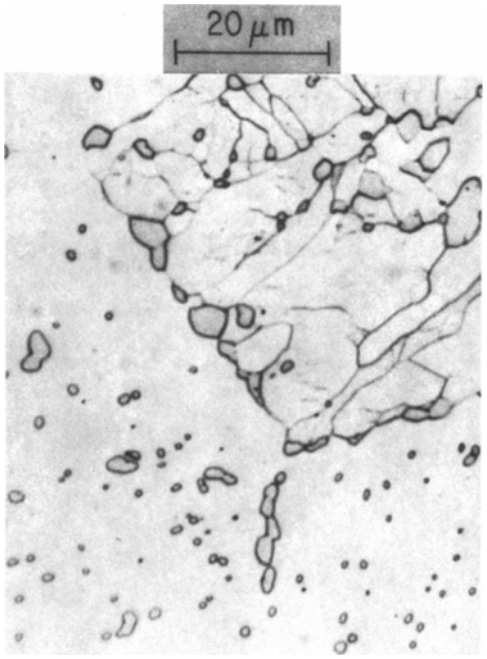

Fig. 19—Partial recrystallization in Fe-0.18 pct C martensite tempered 96 hr at 600°C (1112°F) (light micrograph).[12]

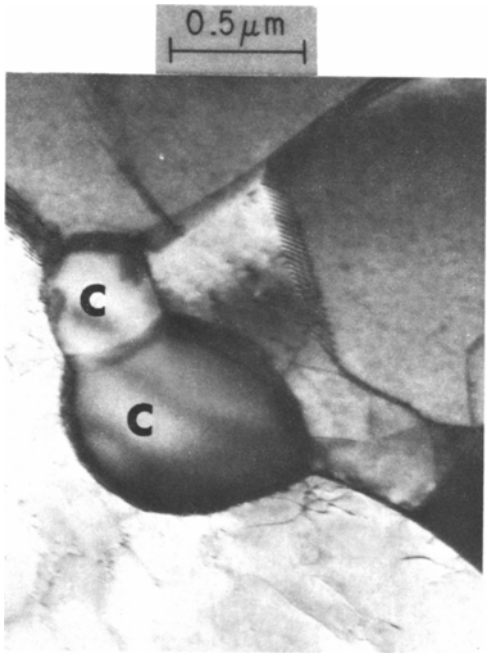

Fig. 20—Pinning of grain boundaries by Fe_3C in Fe-0.18 pct C martensite tempered 96 hr at 600°C (1112°F) (electron transmission micrograph).[12]

(1112°F) and which replace cementite because of their greater stability are discussed in a later section.

DECOMPOSITION OF RETAINED AUSTENITE

The decomposition of retained austenite, if any, occurs at tempering temperatures of 200° to 300°C (392° to 572°F). The decomposition reaction is the formation of bainite. It is sometimes referred to as the second stage of tempering. Retained austenite is present in appreciable quantities in low-alloy steels only when the carbon content exceeds 0.4 pct, see Fig. 4. Therefore, this reaction is important only in medium- or high-carbon steels and is not discussed further here. Lutts[31] has reviewed the data on the second stage of tempering as well as the data on the first and third stages of tempering for work prior to 1963.

RECOVERY AND RECRYSTALLIZATION

It is difficult to tell when recovery of the defect structure begins during the tempering of martensite, but certainly it becomes an important feature of the tempering process above 400°C (750°F). Recrystallization can occur at 600° to 700°C (1112° to 1292°F). The

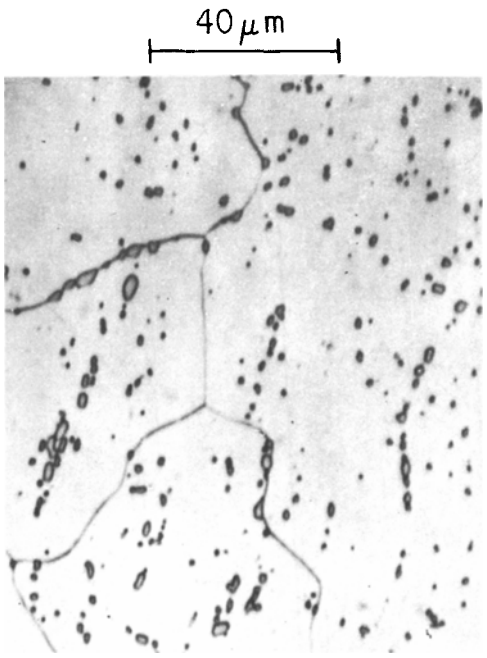

Fig. 21—Completely recrystallized structure in Fe-0.18 pct C martensite tempered 8 hr at 700°C (1292°F).[12]

as-quenched structure of lath martensite contains low-angle dislocation cells and high-angle lath boundaries, Fig. 1. During recovery, the cell boundaries and the random dislocations contained between them are annihilated, and a fine-grained, acicular structure is developed, as shown in Figs. 17 and 18. Recrystallization occurs more readily in low- than in high-carbon steels because the recrystallization process is inhibited by the pinning action of carbides on the boundaries, as shown in Figs. 19 and 20. The structure obtained after long tempering at 700°C (1292°F), shown in Fig. 21, consists of ferrite grains with carbides scattered throughout. After recrystallization is complete, growth of carbide particles and of ferrite grains are the only kinetic processes that continue. The recovery and recrystallization processes in low-carbon martensite have been studied recently by Speich[12] and by Galibois and Dubé.[32,33] Leslie *et al.*[34] have studied the recrystallization of shock-hardened iron which has a defect structure similar to martensite. These results are compared with the recrystallization of cold-worked iron in Fig. 22. The shock-hardened iron recrystallizes at shorter times than the cold-worked iron, indicating it has more stored energy than iron cold-worked 90 pct.

SECONDARY HARDENING

In plain-carbon steels, as in Fe-C alloys, there is a progressive softening accompanied by an increase in ductility as quenched martensite is tempered in the range 100° to 700°C (212° to 1292°F). The hardness changes little at 100°C (212°F) because most of the carbon segregation processes are completed during quenching, although sometimes a small hardness increase is observed in steels of higher carbon content. This usually is attributed to increased carbon segregation to dislocations, as discussed by Ansell and coworkers.[35-37] In higher-carbon steels the formation

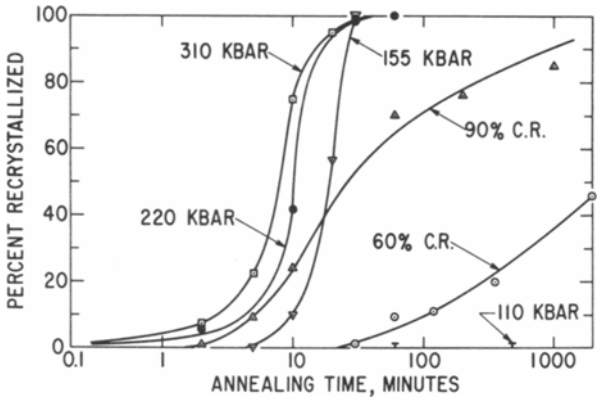

Fig. 22—Recrystallization of shock-hardened iron at 500°C (932°F).[34]

of ϵ-carbide at 150° to 250°C (302° to 482°F) results in a hardness decrease. This step is absent in low-carbon steels because of the reasons previously discussed. The formation of a Widmanstätten array of Fe_3C rods at 300° to 400°C (572° to 752°F) in both low- and high-carbon steels also results in large hardness decreases. Subsequent spheroidization of these carbides and recovery and recrystallization at higher temperatures lead to still further decreases in hardness. The complete process of tempering in iron-carbon martensites is summarized in Fig. 23.

If, however, carbide-forming alloying elements such as Ti, Mo, V, or W are added to the steel, a further and important strengthening reaction occurs in the temperature range from 500° to 600°C (932° to 1112°F). This is called secondary hardening or sometimes the fourth stage of tempering. As a result of this reaction, hardness approaching that of the as-quenched alloy can be achieved. An example from the work of Kuo[38] is shown in Fig. 24. This strengthening is a result of the replacement of coarse particles of Fe_3C, which dissolve, by a fine dispersion of alloy carbides such as TiC, V_4C_3, Mo_2C, and W_2C. Chromium additions result in a retardation in softening, but little or no secondary hardening because Cr_7C_3 coarsens very rapidly at 550°C in contrast to the more stable carbides such as Mo_2C.[38] A large number of different alloy carbides are possible. These form initially as very fine coherent precipitates, primarily on the dislocations inherited from the as-quenched martensite. Their small size and fine dispersion compared to the Fe_3C particles are a result of the smaller distances over which substitutional alloying elements may diffuse compared to carbon. The replacement of a coarse Fe_3C dispersion by a fine dispersion of $(Mo, Cr)_2C$ at higher temperatures is illustrated in Figs. 25 and 26 for a 10 pct Ni-8 pct Co-2 pct Cr-1 pct Mo-0.12 pct C steel.[39] The $(Mo, Cr)_2C$ precipitates are almost entirely nucleated at dislocation sites. At peak hardness Mo_2C needles are typically only 100Å long and about 15Å in diam. Vanadium carbide forms as thin plates on {100} planes in the martensite. These plates are only about 100Å in diam and about 10Å thick. Such secondary hardening reactions have been extensively studied by Honeycombe and others.[40-43]

The secondary hardening reaction can be made even more effective by further alloying additions. In particular, small concentrations (less than 0.1 pct) of strong carbide formers such as niobium increase the peak

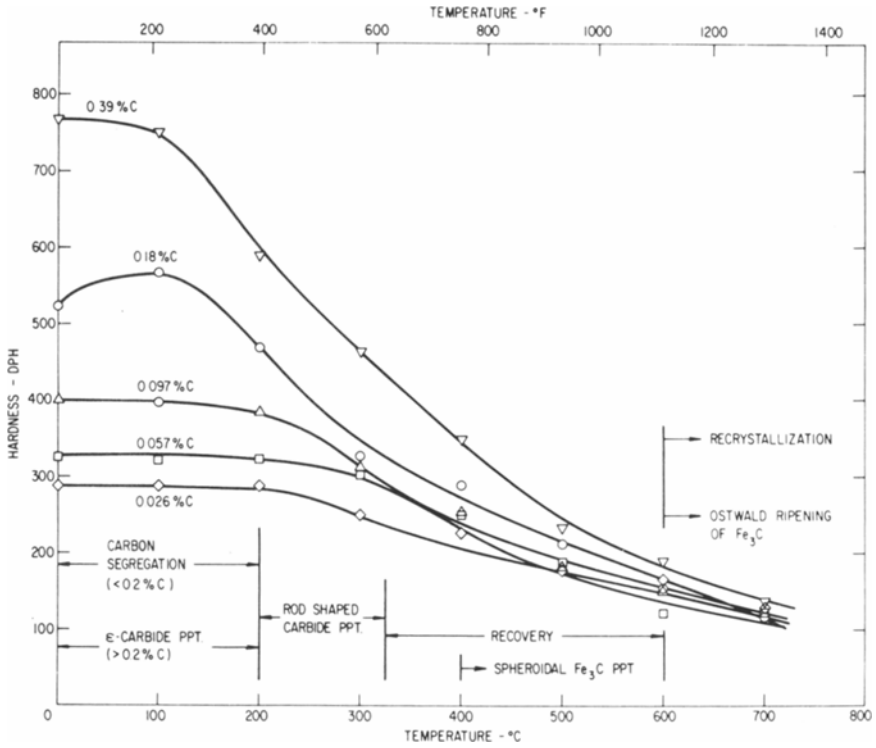

Fig. 23—Hardness of iron-carbon martensites tempered 1 hr at 100° to 700°C (212° to 1292°F).[12]

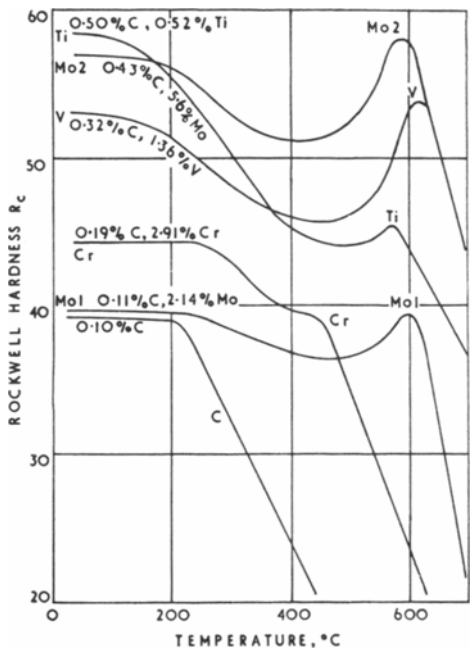

Fig. 24—Secondary hardening of 0.1 to 0.4 pct C steels with additions of Mo, Ti, V, and Cr.[38]

Fig. 25—Coarse dispersion of Fe_3C in 10 pct Ni-8 pct Co-2 pct Cr-1 pct Mo-0.12 pct C steel tempered 1 hr at 426°C (800°F).[39]

hardness substantially and tend to delay overaging. This effect is due primarily to the formation of a fine dispersion of a second carbide phase, NbC. These particles seem to form without regard to the preexisting dislocations.[41]

Some elements do not directly form carbides but affect the secondary hardening reaction indirectly. For instance, cobalt additions to steels are known to produce a higher secondary hardening peak and to retard softening.[44] The exact mechanism for this cobalt effect is still in doubt but in secondary hardening steels where the alloy carbide is dislocation nucleated a major effect of cobalt may be in preventing recovery of the dislocation substructure during tempering.[39,45] This provides more nucleation sites and a finer dispersion of precipitate. Cobalt also increases the activity of carbon in ferrite[46] which favors formation of a fine precipitate dispersion because of the resultant higher supersaturation. Also, cobalt produces a small solid solution strengthening effect.[45]

Some of the effects of Cr, Mo, and Co on the tempering behavior of a 10 pct Ni-0.12 pct C steel are illustrated in Fig. 27. As in the work of Kuo,[38] chromium

retards softening but does not give a secondary hardening peak, which is only present when molybdenum is added to the steel. Cobalt increases the yield strength even when no secondary hardening occurs but has a much more pronounced effect when a secondary hardening precipitate is formed because of the reasons previously discussed.

Secondary hardening is of considerable interest not only because it retards softening but also because the fine dispersion of alloy carbide promotes toughness. The effect of tempering 10 pct Ni-8 pct Co-2 pct Cr-1 pct Mo steels for different times and at different temperatures is illustrated in Fig. 28. The toughness of these steels increases as the tempering time increases because of the dissolution of a coarse dispersion of cementite similar to that shown in Fig. 25 and its replacement by the fine alloy carbide dispersion shown in Fig. 26. Small alloy carbides do not nucleate voids as easily as the larger cementite particles and the toughness increases. It is interesting to note that for short tempering times the toughness continues to increase even though the yield strength also increases. During this period coarse Fe_3C precipitates are dissolved and fine $(Mo, Cr)_2C$ carbides are formed. For longer tempering times the more normal behavior occurs by which the yield strength decreases because of overaging and the toughness increases. During this period, only the coarsening of $(Mo, Cr)_2C$ carbide occurs. An optimum tempering time is thus required to achieve the maximum toughness for a given yield strength.

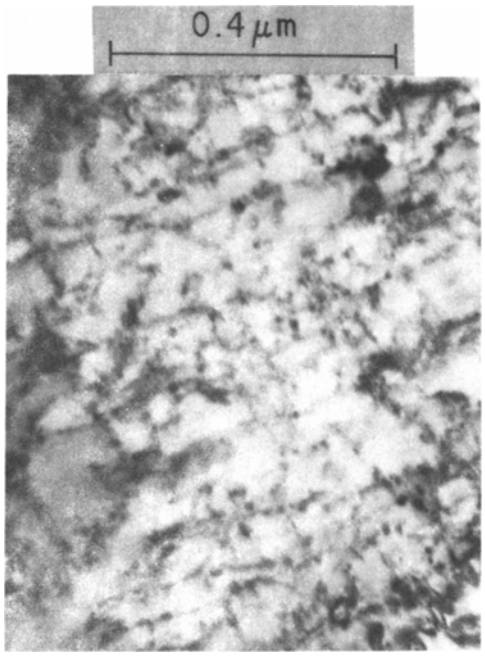

Fig. 26—Fine dislocation-nucleated dispersion of $(Mo, Cr)_2C$ in 10 pct Ni-8 pct Co-2 pct Cr-1 pct Mo-0.12 pct C steel tempered 12 hr at 510°C (950°F).[39]

EMBRITTLEMENT DURING TEMPERING

Martensite is tempered to improve its ductility, but tempering must be done with care, or ductility will not be improved. As shown in Fig. 29, if tempering is done between 230° and 370°C (450° and 700°F), embrittlement can occur in a number of different AISI steels.[47] This phenomenon is termed "500°F embrittlement". It is believed to be associated with a critical carbide morphology present when Fe_3C first forms. It may be caused by film-like carbides precipitated on grain boundaries and subboundaries.[48] This phenomenon is a serious handicap to the development of optimum strength and toughness. If one uses a low-alloy steel containing silicon, this problem of 500°F embrittlement can be avoided. Silicon inhibits the tempering of martensite. When 1.5 pct or more silicon is present, the rate of softening becomes zero at about 250°C (500°F). Silicon inhibits the tempering of martensite by two processes: 1) it inhibits the growth of carbide particles, and 2) it expands the range of temperature in which ϵ-carbide is stable.

If an alloying element is more soluble in cementite than in ferrite, as are Mn, Mo, Cr, and W, it is not

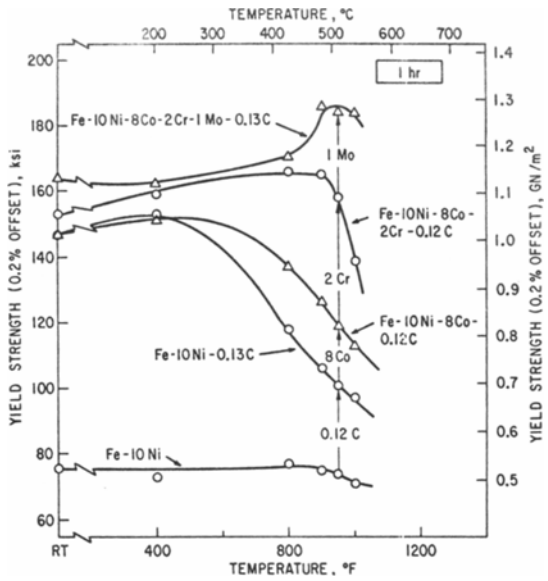

Fig. 27—Effect of C, Co, Cr, and Mo on tempering of 10 pct Ni steels.[39]

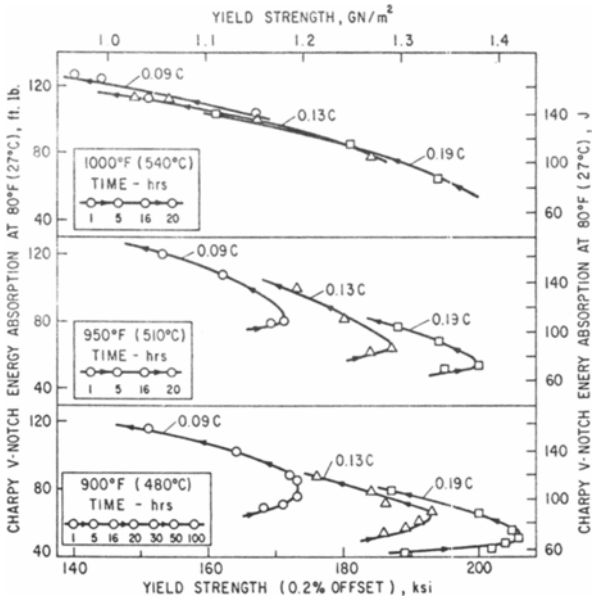

Fig. 28—Fracture toughness and yield strength of 10 pct Ni-8 pct Co-2 pct Cr-1 pct Mo steels with various carbon contents and tempering treatments.[39]

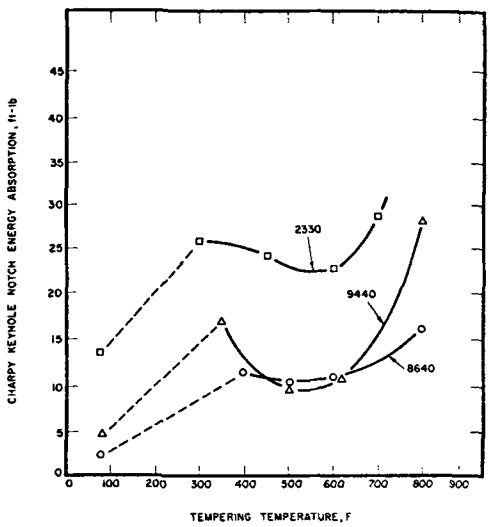

Fig. 29—500°F embrittlement in AISI 2330, 8640, and 9440 steels.[47,48]

likely to have a pronounced effect on the rate of growth of carbides precipitated from martensite, although it may affect the structure, nucleation sites and rate of nucleation of the carbide. Alloying elements insoluble in the carbide, such as silicon, may have a very large effect upon rate of growth of carbides. Owen[49] proposed that the technologically important inhibition of the tempering of martensite by silicon was due to the rejection of silicon by the growing carbide particles. The buildup of silicon around the growing particle causes an increase in the activity of carbon in this region, thereby decreasing the flux of carbon to the particle and decreasing the rate of growth. Keh and Leslie[50] determined the effect of silicon on the rate of growth of carbides, with the results shown in Fig. 30. The rate of growth is compared with the growth of carbides in an Fe-Mn-C alloy. The effects were measured in ferrite, not in martensite, but that is unimportant. The effect of silicon is quite striking. During aging at 200°C (392°F), the carbides in the Fe-Mn-C alloy (Fe_3C) grew to a maximum dimension of 14,500Å in 20 min. In the Fe-Si-C alloy, the carbides, which are not Fe_3C, grew initially at 200°C (392°F) at about the same rate as in the Fe-Mn-C alloy, but soon reached a maximum size characteristic of the aging temperature, after which growth ceased. The maximum size was about 2000Å at 100°C (212°F), 3000Å at 200°C (392°F) and 8000Å at 300°C (572°F). These temperatures cover the range in which silicon inhibits the tempering of martensite. It seems probable that the effective mechanism is that proposed by Owen, wherein each growing carbide, whether precipitated in ferrite or martensite, is encapsulated by a high concentration of silicon, which eventually nearly halts the migration of carbon to or from the particle. If this is correct, the movement of silicon atoms away from the growing carbide particle must be aided by some means that have yet to be elucidated.

Recently it was reported that during the tempering of a 0.5 pct C, 0.8 pct Mn, 2.0 pct Si steel, ϵ-carbide precipitated at 150°C (302°F), Fe_3C at 500°C (932°F), but that at 300°C (572°F) a new hexagonal, high-silicon (9 pct) carbide, called γ, was precipitated.[51] Gamma is supposedly an intermediate carbide between ϵ-carbide and Fe_3C. Confirmation by others of this interesting claim is desirable.

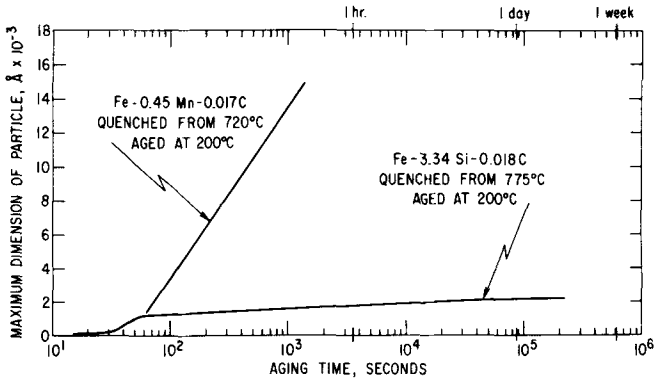

Fig. 30—Effect of silicon on rate of growth of carbide particles during the quench-aging of ferrite.[50]

The last topic we will discuss is temper embrittlement. This occurs in quenched and tempered steels when they are held in or slowly cooled through the temperature range 370° to 565°C (700° to 1050°F). The embrittlement—a loss of cohesion at prior austenite grain boundaries—is believed to be caused by segregation of antimony and phosphorus and, to a lesser extent, of arsenic and tin to prior austenite grain boundaries during austenitizing of the steel.[52-54]

The susceptibility of a steel to temper embrittlement is also enhanced by segregation of alloying elements, particularly manganese and chromium, to prior austenite boundaries. Apparently the embrittling elements are arranged near the grain boundaries and move to the embrittling configuration only in the temperature range 370° to 565°C (700° to 1050°F). Below about 370°C (700°F) the mobility of the embrittling elements is restricted and above about 565°C (1050°F) they return to the unembrittling configuration. As a result the embrittlement is characterized by a "C" curve, with a nose between 500° and 550°C (932° and 1022°F). Embrittled steels can have their ductility restored by heating at temperatures above 565°C (1050°F), for a few minutes at 593°C (1100°F), for example. There is an enormous amount of information available on the subject of temper embrittlement, but the phenomenon is so complex that no simple model has been proposed that satisfactorily explains all its features.

REFERENCES

1. M. A. Grossman and E. C. Bain: *High Speed Steel*, John Wiley, London, 1931.
2. E. C. Bain: *Functions of the Alloying Elements in Steel*, ASM, 1939, Cleveland, Ohio; 2nd Edition co-authored with H. W. Paxton, 1961.
3. E. C. Bain: *J. Iron Steel Inst.*, 1955, vol. 181, pp. 193-212.
4. G. R. Speich and P. R. Swann: *J. Iron Steel Inst.*, 1965, vol. 203, pp. 480-85; G. R. Speich and H. Warlimont: *J. Iron Steel Inst.*, 1968, vol. 206, pp. 385-92.
5. A. R. Marder and G. Krauss: *Trans. ASM*, 1967, vol. 60, pp. 651-59; *Trans. ASM*, 1969, vol. 62, pp. 957-63.
6. J. D. Embury, A. S. Keh, and R. M. Fisher: *Trans. TMS-AIME*, 1966, vol. 236, pp. 1252-60.
7. G. R. Speich: private communication, E. C. Bain Laboratory, U. S. Steel Corp., Monroeville, Pa., April 1971.
8. A. B. Greninger and A. R. Troiano: *Trans. ASM*, 1942, vol. 30, pp. 1-26.
9. M. J. Bibby and J. Gordon Parr: *J. Iron Steel Inst.*, 1964, vol. 202, pp. 100-04.
10. M. Cohen: *Japan Inst. Metals*, Spec. Supp., 1968, vol. 9, pp. XXIII-XXIX; D. Kalish and M. Cohen: *Mater. Sci. Eng.*, 1970, vol. 6, pp. 156-66.
11. J. D. Baird: *Metals Mater.*, 1971, vol. 5, pp. 1-18; *Iron Steel*, 1963, vol. 36, p. 186.
12. G. R. Speich: *Trans. TMS-AIME*, 1969, vol. 245, pp. 2553-64.

13. W. S. Owen, E. A. Wilson, and T. Bell: *High Strength Materials,* John Wiley, pp. 167-205, New York, 1965.
14. G. V. Kurdjumov: *Rev. Met. Mem. Soc.,* 1967, vol. 64, pp. 99-110.
15. G. V. Kurdjumov: *Fiz. Metal. Metalloved.,* 1967, vol. 24, pp. 909-17.
16. S. O. Suvorova, V. I. Sarrak, and R. I. Entin: *Fiz. Metal. Metalloved.,* 1964, vol. 17, pp. 105-11; *Doklady Akad. Nauk SSSR,* 1963, vol. 4, p. 156.
17. J. M. R. Genin and P. R. Flinn: *Trans. TMS-AIME,* 1968, vol. 242, pp. 1419-30.
18. P. G. Winchell and M. Cohen: *Trans. ASM,* 1962, vol. 55, pp. 347-61.
19. V. I. Izotov and L. M. Utevskii: *Fiz. Metal. Metalloved.,* 1968, vol. 25, pp. 98-100.
20. A. G. Khachaturyan: *Fiz. Tverd. Tela.,* 1967, vol. 9, pp. 2861-69; *Doklady Akad. Nauk SSSR,* 1965, vol. 165, pp. 551-54.
21. R. A. Johnson: *Acta Met.,* 1967, vol. 15, pp. 513-17.
22. R. A. Johnson: *Acta Met.,* 1965, vol. 13, pp. 1259-62.
23. D. W. Hoffman: *Acta Met.,* 1970, vol. 13, pp. 819-33.
24. M. G. H. Wells: *Acta Met.,* 1964, vol. 12, pp. 389-99.
25. F. W. Langer: An Investigation of the Quench Aging Process in Iron, Department of Metallurgy, Technical University, Denmark, 1967; *Metal Sci. J.,* 1968, vol. 2, pp. 59-66.
26. H. W. Wagenblast and R. Glenn: *Met. Trans.,* 1970, vol. 1, pp. 2299-2304.
27. W. C. Leslie and A. S. Keh: *Mechanical Working of Steel II,* pp. 337-77, Gordon and Breach, N. Y., 1965.
28. H. Ino, T. Mouya, E. Fujita, Y. Maeda, Y. Oni, and Y. Inokuti: *J. Phys. Soc. Japan,* 1968, vol. 25, pp. 88-99.
29. K. H. Jack and S. Wild: *Nature,* 1966, vol. 212, pp. 248-50.
30. W. C. Leslie, R. M. Fisher, and N. Sen: *Acta Met.,* 1959, vol. 7, pp. 632-44.
31. A. Lutts: *Rev. Univ. Mines,* 1963, vol. 19, pp. 325-41.
32. A. Galibois and A. Dubé: *Can. Met. Quart.,* 1964, vol. 3, pp. 321-43.
33. A. Galibois and A. Dubé: *Can. Met. Quart.,* 1967, vol. 6, pp. 21-36.
34. W. C. Leslie, E. Hornbogen, and G. E. Dieter: *J. Iron Steel Inst.,* 1962, vol. 200, pp. 622-33.
35. G. S. Ansell and A. Arrot: *Trans. TMS-AIME,* 1963, vol. 227, pp. 1080-82.
36. G. S. Ansell and E. M. Breinan: *Trans. ASM,* 1965, vol. 58, pp. 110-13.
37. G. S. Ansell, V. I. Lizunov, and R. W. Messler: *Jap. Inst. Metals* Spec. Supp., 1968, vol. 9, pp. 933-39.
38. K. Kuo: *J. Iron Steel Inst.,* 1956, vol. 184, pp. 258-68.
39. G. R. Speich, D. Dabkowski, and L. F. Porter: *Met. Trans.,* 1972, to be published.
40. R. W. K. Honeycombe and A. K. Seal: *Precipitation Processes in Steels,* Iron Steel Inst., Spec. Rep. No. 64, 1959, pp. 44-56.
41. R. W. K. Honeycombe: *Metallography 1963,* Iron Steel Inst., Spec. Rep. No. 80, 1964, pp. 246-305.
42. R. W. K. Honeycombe: *Metallurgical Developments in High-Alloy Steels,* Iron Steel Inst., Spec. Rep. No. 86, 1964, pp. 1-14.
43. R. W. K. Honeycombe, H. J. Harding, and J. T. Irani: *High Strength Materials,* pp. 213-50, John Wiley, 1965.
44. V. K. Chandhok, J. P. Hirth, and E. J. Dulis: *Trans. ASM,* 1963, vol. 56, pp. 677-91.
45. J. T. Michalak and G. R. Speich: unpublished work, E. C. Bain Laboratory, U. S. Steel Corp., Monroeville, Pa.
46. V. K. Chandhok, J. P. Hirth, and E. J. Dulis: *Trans. TMS-AIME,* 1962, vol. 224, pp. 858-64.
47. R. L. Rickett and J. M. Hodge: *Proc. ASTM,* 1951, pp. 931-44.
48. L. F. Porter: *Metallurgical Factors Affecting Toughness,* ASM Seminar, Houston, Texas, 1969.
49. W. S. Owen: *Trans. ASM,* 1954, vol. 46, pp. 812-29.
50. A. S. Keh and W. C. Leslie: *Materials Science Research,* vol. 1, Plenum Press, N. Y., 1963, pp. 208-50.
51. R. A. Tewau and P. R. Dahr: *J. Iron Steel Inst.,* 1970, vol. 208, pp. 87-88.
52. B. C. Woodfine: *J. Iron Steel Inst.,* 1953, vol. 173, pp. 229-39.
53. J. R. Low: *Fracture of Engineering Materials,* pp. 127-42, ASM, Cleveland, Ohio, 1959.
54. P. A. Restaini and C. J. McMahon: *Trans. ASM,* 1967, vol. 60, pp. 699-706.